JOURNAL OF MATERIALS SCIENCE 32 (1997) 2811–2819

The oxidation behaviour of low-temperature heat-treated carbon fibres

L. R. ZHAO*, B. Z. JANG
Materials Research and Education Center, Auburn University, AL 36849, USA

The oxidation behaviour of partially carbonized polyacrylonitrile fibres was studied primarily by both dynamic and isothermal thermogravimetric analysis. These fibres, referred to as quasi-carbon fibres (QCFs), were obtained by pyrolysis of a polyacrylonitrile precursor at a heat-treatment temperature (HTT) ranging from 400–950 °C. Results indicated that QC fibres exhibited increased thermal stability with increasing HTT. The oxidation behaviour was strongly related to the microstructure of QC fibres. An empirical model was developed to simulate the real oxidation process. Two different oxidation mechanisms were operational in QC fibres; one with a more moderate oxidation rate and the other with an auto-acceleration effect. Only the QC fibres that were heat treated above 650 °C to develop an extended two-dimensional graphite-like structure, exhibited an auto-acceleration effect.

1. Introduction

Partially carbonized polyacrylonitrile (PAN) fibres (or quasi-carbon fibres, QCFs) have been shown to exhibit semiconducting characteristics and acceptable mechanical properties [1–4]. Based on unusual switching behaviour and anomalous semiconductor–metal transition observed in these semiconducting fibres, the existence of possible excitonic superconducting domains has been speculated [5, 6]. Their unique physical and chemical nature makes them useful as potential functional materials, such as thermal-type infrared detectors and varistors [7–9], for future high-tech applications. One of the most important concerns, with respect to such applications, is the need for good oxidation resistance; to restrain their affinity with oxygen and other oxidizing gases. Therefore, a method needs to be developed for predicting the reactivity of these carbon materials at elevated temperatures and for relating this effect to engineering design properties.

The oxidation behaviour of conventional carbon fibres has been studied extensively [10–14]. Different types of carbon fibres were oxidized in different fashions, depending on the precursor fibre type and fibre processing conditions. Ismail [10], in studying the oxidation of carbon fibres and carbon fabrics at a temperature in the range 600–950 °C, found that the oxidation rate was related to the crystallinity of the fibre. The graphitized fibre, having a well-defined X-ray diffraction pattern, exhibited the typical autocatalytic reaction characteristic. A similar result was observed with an intermediate-modulus carbon fibre (IM-7) by Trumbauer *et al.* [15], and a maximum reaction rate appeared at about 40% carbon burn-off (BO) due to a change in the active surface area (ASA) of the fibre. The fibre diameter also varied significantly during the oxidation process. The activation energy of carbon BO was reported to lie in the range 140–190 kJ mol^{-1} [14, 16, 17] for a test temperature range of 500–850 °C. According to Yin *et al.* [14], the oxidation of the carbon fibre was a reaction-controlled process, even though gas diffusion made some contribution to the overall reaction rate. Thus far, little research has been reported on the oxidation behaviour of partially carbonized fibres which are obtained by heat treatment at a temperature below 1000 °C. Reported here are the results of our efforts to investigate the oxidation kinetics of these QC fibres in the hope of developing a model to simulate the real oxidation process and to obtain an improved understanding of the relationship between the structure and the oxidation behaviour of QC fibres.

2. Experimental procedure

2.1. Fabrication of QC fibres

All of the QC fibres used in this study were prepared in our laboratory by a method reported earlier [3]. The PAN-based copolymer fibre, in the form of a tow containing 6000 filaments, was utilized as the fibre precursor to obtain partially carbonized products. The precursor was stabilized in air at a temperature in the range of 210–230 °C for 2.5 h to form the OXPAN fibre. Then, the OXPAN fibre was pyrolyzed at a desired temperature ranging from 400–950 °C for 1 h to produce various QC fibres. Thus, fibres heat treated at HTTs of 400, 500, 650, 800 and 950 °C were labelled QCF-400, QCF-500, QCF-650, QCF-800 and

* Author to whom all the correspondence should be addressed. *Present address*: Therm–O–Disc, Inc., Advanced Technology Department, 1320 S. Main Street, Mansfield, OH 44907, USA.

0022–2461

QCF-950, respectively. For comparison, carbon fibre was also prepared from the OXPAN fibre using an HTT of 1200 °C.

2.2. Oxidation measurement

A Perkin–Elmer TGA-7 thermal analyser was employed for the study of the oxidation of QC fibres. The fibres were chopped to about 0.4 cm length and then placed in a platinum sample holder with all fibres lying in one direction. The weight loss of the fibres was determined by the TGA microbalance with a sensitivity of 0.001 mg. The original weight of each sample for TGA measurement was approximately 3 mg. Both isothermal and dynamic thermogravimetric scans were performed in experiments with an air flow rate of 80 ml min^{-1}. The dynamic TGA scan was carried out with a heating rate of 20 °C min^{-1} from 30–850 °C, while the isothermal TGA scans were conducted in the temperature range 400–650 °C.

3. Results and discussion

3.1. Characterization of QC fibres

Selected material properties of QC fibres are summarized in Table I. With an increased HTT, the QC fibre exhibited an increased density, crystallinity and crystalline size values (L_a and L_c), but a decreased filament diameter. The Young's modulus magnitudes of the QC fibres scaled almost linearly with the pyrolysis temperature, but the QCFs exhibited a decreasing trend in both tensile strength and failure strain up to an HTT of 650 °C, above which both the tensile strength and failure strain of the QC fibres increased with increasing HTT. Further, QC fibres heat treated at a temperature below 950 °C were found to exhibit an electrically semi-conducting behaviour.

Fig. 1 shows scanning electron micrograph observations of the surface texture of QC fibres. The striations along the fibre axis on the fibre surface (QCF-400) can be clearly seen (Fig. 1a). The surface of the QCF-650 became more "ribbed" and "fluted" and the carbonaceous deposits appeared at the fibre surface due to strong chemical reactions, resulting in severe shrinkage in both the longitudinal and transverse directions of the filament (Fig. 1b). After heat treatment at a higher temperature, the fibre tended to reorganize and extend the fused aromatic rings to form a graphite-like structure. Thus, the QCF-950 exhibited a less "fluted" surface (Fig. 1c). A polished cross-sectional area of a fibre bundle (QCF-800) revealed that the QC fibres were elliptical in shape, as shown in Fig. 2.

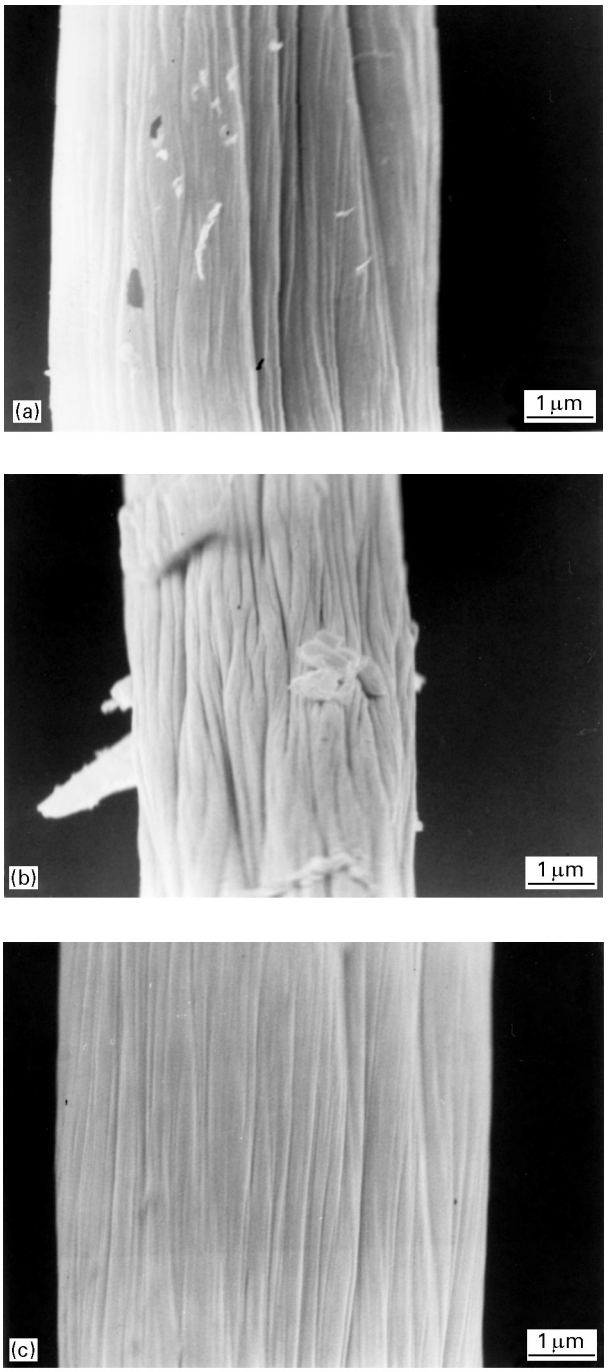

Figure 1 Scanning electron micrographs of texture in QC fibres: (a) QCF-400, (b) QCF-650, and (c) QCF-950.

TABLE I Properties of QC fibres

Properties	QCF-400	QCF-500	QCF-650	QCF-800	QCF-950	Carbon fibre
Diameter (μm)	9.86	9.40	8.43	8.12	7.44	6.83
Density (g cm^{-3})	1.48	1.61	1.75	1.78	1.80	1.81
Tensile stress (MPa)	162.2	134.4	146.0	197.6	288.4	406.4
Tensile modulus (GPa)	17.42	39.84	71.96	105.6	133.0	187.3
Ultimate elongation (%)	1.061	0.339	0.195	0.205	0.234	0.467
Stacking size, L_c (nm)	1.16	1.19	1.24	1.27	1.33	2.15
Layer width, L_a (nm)	2.05	2.11	2.19	2.25	2.35	3.81
Electrical resistivity, ρ (Ω cm)	7.064	3.736	0.030	− 1.725	− 2.554	− 2.809

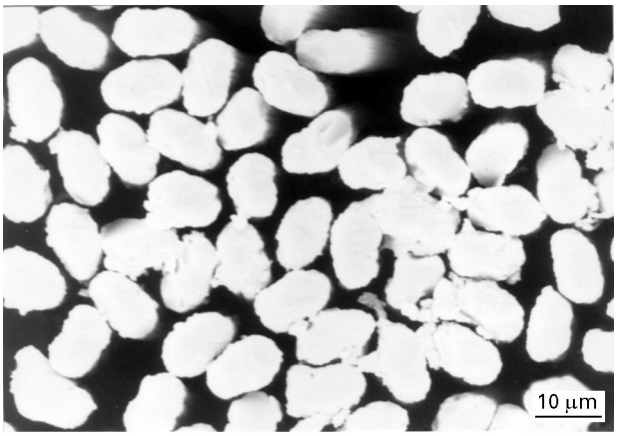

Figure 2 Scanning electron micrograph of a cross-sectional area of a QCF-800 bundle.

3.2. The dynamic TGA scan

Fig. 3 illustrates the TGA results obtained by using the dynamic thermal scan mode on the PAN, OXPAN, and QC fibres which were obtained by pyrolysing at different temperatures, each for 1 h. Mass loss of the PAN fibre appeared at 260 °C due to cyclization of the original PAN structure. The mass loss onset temperature of the OXPAN fibre was at 330 °C, which was considered to be associated with oxidation degradation. The mass loss of QCFs began at higher temperatures, 565.3, 606.9, 665.5 °C for the QCF-400, QCF-500 and QCF-950, respectively, and the slope of the mass loss versus temperature curve became steeper with increasing HTT; suggesting that the higher the fibre HTT, the less was the initial fibre active surface area (ASA) and the higher the oxidation resistance. This is probably due to the formation of a more ordered structure. Thus, QCFs exhibited increased thermal stability with increased HTT.

3.3. The isothermal scan

3.3.1. Oxidation rate

Figs 4–8 demonstrate the relationship between the weight loss percentage (%) and oxidation time for five QCF samples (QCF-400, QCF-500, QCF-650, QCF-800 and QCF-950), exposed to an air atmosphere over a temperature range of 400–650 °C. All QCF samples showed an increased reaction rate with an increase in the oxidation temperature. At a specific temperature (e.g. 500 °C), the reaction rate was reduced with increasing HTT (Fig. 9), indicating that the thermal stability of the QC fibre was raised with increased HTT, which was consistent with the data previously obtained from the dynamic TGA scan. The reactions of the QC fibre with oxygen were quite complicated, due to a finite amount of nitrogen, oxygen and hydrogen existing in the structure of the QC fibres; especially in those QC fibres that were heat treated at a lower temperature. However, the overall chemical reactions can be expressed as

$$[\mathrm{QCF}] + \mathrm{O_2} \rightarrow \mathrm{CO_2} + \mathrm{H_2O} + [\text{N-containing oxide}] \quad (1)$$

$$[\mathrm{QCF}] + \mathrm{O_2} \rightarrow \mathrm{CO} + \mathrm{H_2O} + [\text{N-containing oxide}] \quad (2)$$

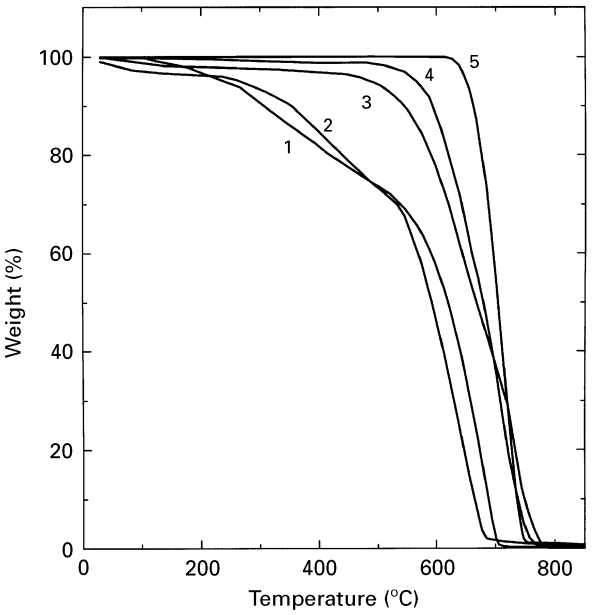

Figure 3 Dynamic scan data of (1) PAN, (2) OXPAN and QC fibres (3) QC-400, (4) QC-500, and (5) QC-950.

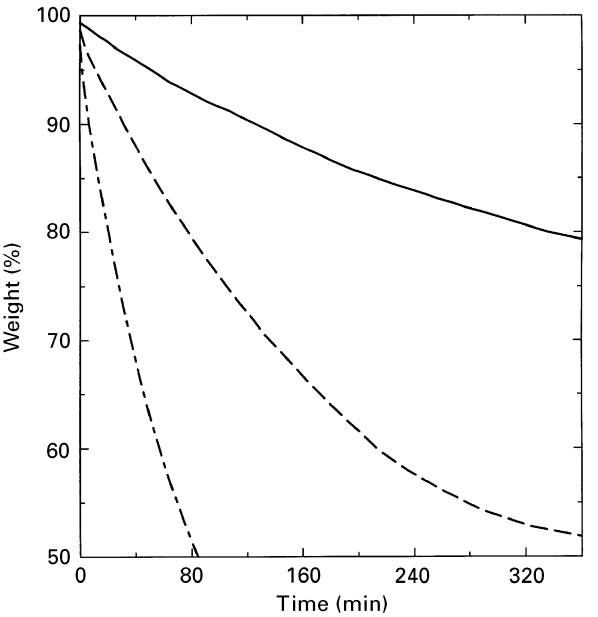

Figure 4 Isothermal scan data of QC-400 at (——) 400 °C, (– – –) 450 °C, and (— - —) 500 °C.

Because there was ample oxygen for the oxidation process, the effective reaction rate was considered to be of a fixed order in the measured temperature range. Thus, the reaction rate, r, can be written as

$$r = kA \quad (3)$$

where A is the ASA of the fibre and k is a material constant, or

$$r = \mathrm{d}m/\mathrm{d}t = -Rm \quad (4)$$

From the carbon burn-off (BO) percentage, $x = (m_0 - m)/m_0$, one may obtain an equation, as follows, by rearranging Equation 4

$$R = [1/(1-x)]\,\mathrm{d}x/\mathrm{d}t = [1/(1-x)]r \quad (5)$$

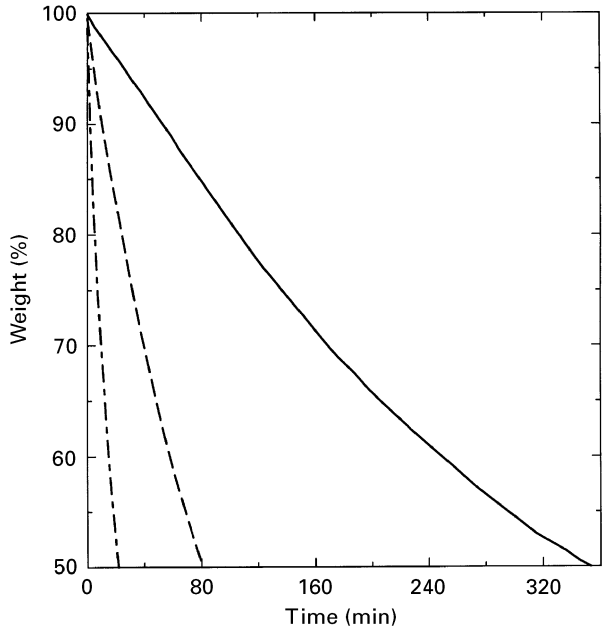

Figure 5 Isothermal scan data of QC-500 at (——) 450 °C, (– – –) 500 °C, and (— · —) 550 °C.

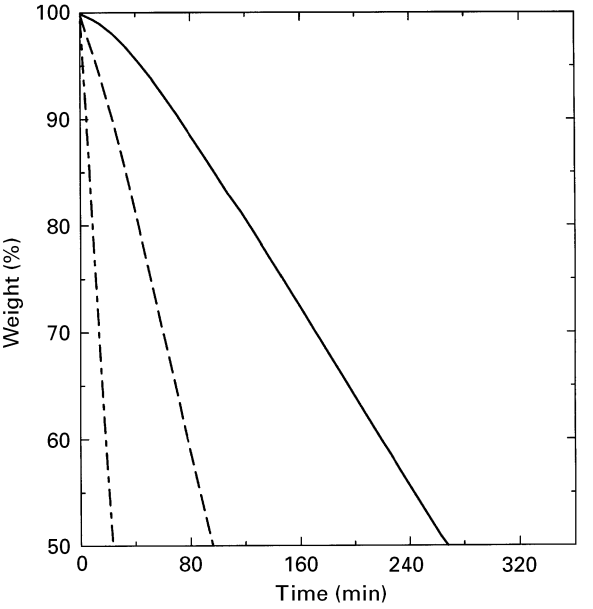

Figure 7 Isothermal scan data of QC-800 at (——) 500 °C, (– – –) 550 °C, (— · —) 600 °C.

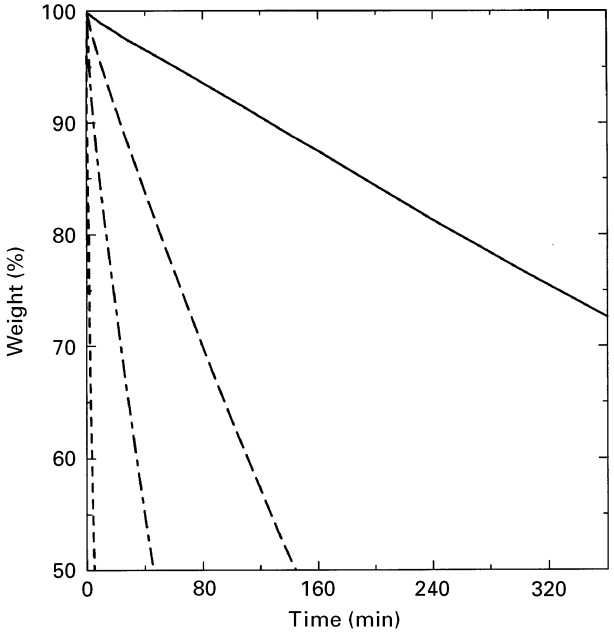

Figure 6 Isothermal scan data of QC-650 at (——) 450 °C, (– – –) 500 °C, (— · —) 550 °C, (· · ·) 650 °C.

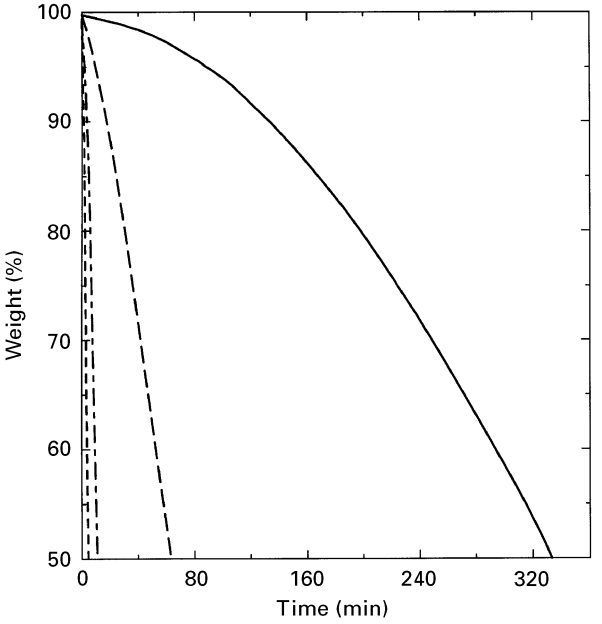

Figure 8 Isothermal scan data of QC-950 at (——) 500 °C, (– – –) 550 °C, (— · —) 600 °C, (· · ·) 650 °C.

where m is the amount of the QC fibre at time t, m_0 is the initial amount of the QC fibre and R is defined as a specific reaction rate or reactivity which is constant for a fixed BO percentage, x. Equations 3 and 5 will be used to discuss and evaluate the oxidation process in the following sections

Further analysis of the isothermal scan data indicates that the carbon BO rate, r, strongly depends upon the weight loss percentage, $1 - x$, or the carbon BO percentage, x, as indicated in Fig. 10. The QC fibres could be divided into two categories according to the HTT. For the first category, QC fibres heat treated at a temperature below 650 °C, the r values decreased with their x values. At the early stage of carbonization, the graphite-like structure in the QC fibres was not well developed, and the ladder and partially cross-linked molecular chains in the OXPAN fibres were condensed to form species with a small crystallite size, leaving flaws among the embryonic basal planes. Thus, a larger ASA led to a larger value of reaction rate, r. Owing to the smaller crystallite size and larger ASA than those of the QCF-500, the QCF-400 exhibited a higher initial oxidation rate. With an increase in the reaction time, t, or an increase in the x value, the reduction of the reaction rate in both QCF-400 and QCF-500 could be partially explained as due to a decrease in the m value, as is indicated in Equation 4.

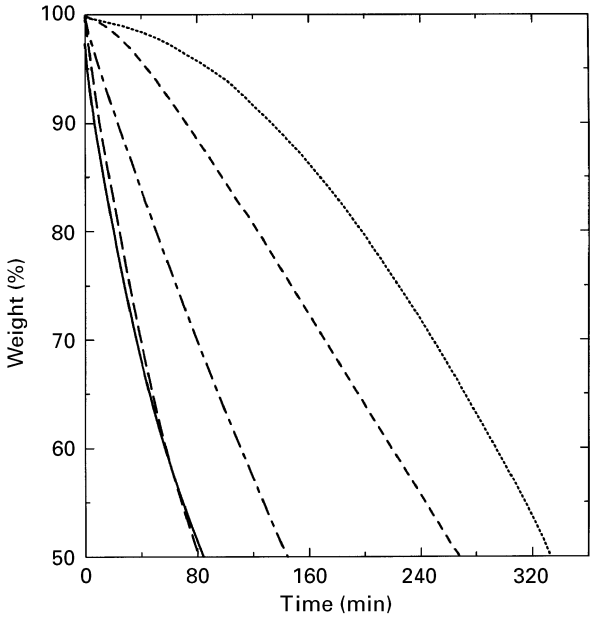

Figure 9 Weight loss versus time curves of various QC fibres at 500 °C: (——) QCF-400, (— — —) QCF-500, (—·—) QCF-650, (– – –) QCF-800, (- - -) 950 °C.

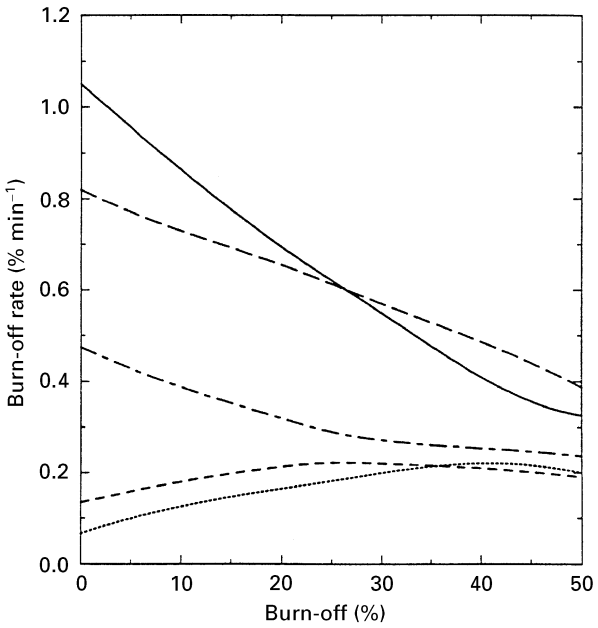

Figure 10 The burn-off rate, r, as a function of burn-off percentage, x, for various QC fibres. For key see Fig. 9.

The second category includes QC fibres heat treated at a higher temperature (QCF-800 and QCF-950). For this category, the r value initially increased with x, then reached a maximum value at a specific value of x (25% and 40% for QCF-800 and QCF-950, respectively), above which the BO rate decreased with x. The effect could be described as an auto-acceleration effect; similar to the result obtained from the carbon fibre [16]. When QC fibres were pyrolysed at well above 650 °C, the graphite-like structure in such QC fibres had the extended two-dimensional molecular chains. The increased crystalline size would result in a decrease in the ASA. Therefore, the QCF-950 initially had the lowest r value. An increased x value implies

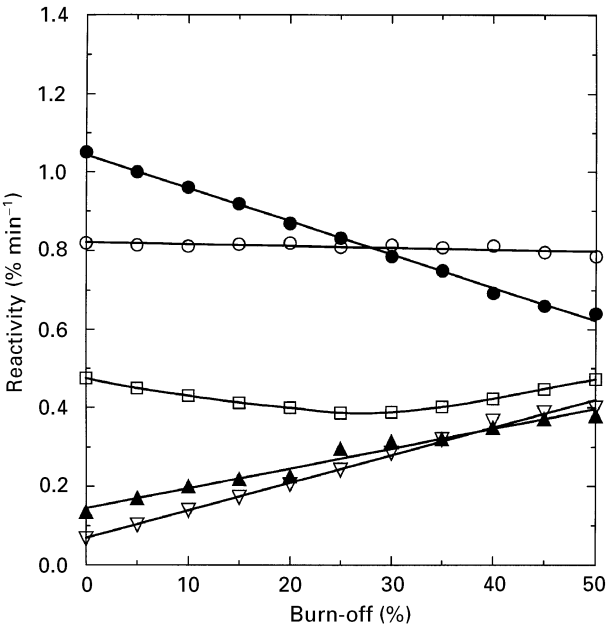

Figure 11 The reactivity, R, as a function of burn-off percentage, x, for various QC fibres: (▽) QCF-950, (▲) QCF-800, (□) QCF-650, (○) QCF-500, (●) QCF-400.

that the oxidation should gradually break off the extended two-dimensional structure to form several smaller species, thereby increasing the ASA of the fibre; thus, the self-catalytic characteristic for the QCF-800 and QCF-950 can be observed. After a critical point, x_c, a situation similar to that occurring in the first category would develop; i.e. the r value decreased with increasing x. Therefore, the oxidation rate of QC fibres is strongly related to the crystalline size, crystallinity, and the ASA.

Fig. 11 illustrates the variation of reactivity, R, with the BO percentage, x at 500 °C for QC fibres heat treated in a temperature range 400–950 °C. Because the R value of all QC fibres, except for the QCF-650, exhibited a linear change with x (up to 50%), the relation between R and x could be used for quantitatively evaluating and analysing the oxidation process. The lines of both the QCF-400 and QCF-500 appear to have a negative slope, while those of the QCF-800 and QCF-950 have positive slopes. The change of the R value with x for the QCF-650 was more complicated. The QCF-650 line shows an initial negative slope at the initial BO stage (x up to 27.5%), above which a positive slope value was observed. The reactivity, R, for all cases, though, can be approximately expressed as

$$R(x) = a + bx \tag{6}$$

where a is the intercept and b the slope of the R versus x lines. The parameter a actually indicates the initial oxidation rate ($x = 0$) of the QC fibres. The larger the value of a, the higher is the rate. The b value reflects the oxidation mechanism. Only a positive b value indicates auto-acceleration occurring in the QC fibres. Both a and b values of various QC fibres are summarized in Table II. By substituting Equation 6 into Equation 5 and solving the integral, the relation can

TABLE II Parameters a and b of QC fibres for simulating oxidation behaviour

QC fibres	a (10^{-2} min^{-1})	b (10^{-2} min^{-1})
QCF-400	1.043	− 0.483
QCF-500	0.822	− 0.048
QCF-650 ($x \leqslant 27.5\%$)	0.468	− 0.338
QCF-650 ($x \geqslant 27.5\%$)	0.259	0.422
QCF-800	0.145	0.504
QCF-950	0.069	0.701

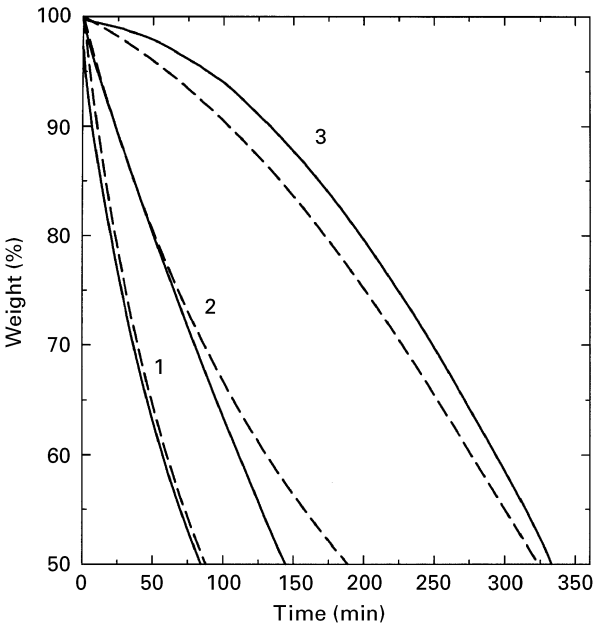

Figure 12 A comparison between (——) real and (— —) simulated oxidation process of QC fibres at 500 °C: (1) QCF-400, (2) QCF-650, (3) QCF-950.

be obtained between the weight loss percentage, $1 - x$, and the oxidation time, t, of QC fibres

$$(1 - x) = (a + b)/[a\exp(a + b)t + b] \qquad (7)$$

Fig. 12 shows a replot of $1 - x$ versus t of QC fibres, using Equation 7. Being in good agreement with experimental data, Equation 7 represents a good simulation of the real oxidation process occurring in the QC fibres.

3.3.2. Activation energy

As stated earlier, the reactivity, R, or the reaction rate, r, is a constant at a specific BO percentage, and only changes with the oxidation temperature. By using the Arrhenius equation

$$r = r_0 \exp(-Q/RT) \qquad (8)$$

or

$$R = R_0 \exp(-Q/RT) \qquad (9)$$

where r_0 or R_0 is a pre-exponential constant, Q is the activation energy of the QC fibre and T is the absolute temperature (K) for the oxidation, the Q value can be obtained statistically from the slope of the $\ln r$ versus $1/T$ line. Selected Arrhenius plots of QC fibres (the QCF-650, in a temperature range 450–650 °C, and the QCF-950, in a temperature range 500–650 °C for various x are shown in Figs 13 and 14, respectively. All lines, in both figures, for different x had almost identical slopes, indicating that the Q value of the QC fibre was not a function of BO percentage, x. For the QCF-650 fibre, the $\ln r_0$ value decreased with increasing x. Owing to auto-acceleration, the reverse situation was observed for the QCF-950 fibre, as seen in Fig. 14, i.e. the $\ln r_0$ value increased with increasing x, up to 40%. The pre-exponential constants (r_0 and R_0) of various QC fibres at different BO stages are summarized in Table III.

The variation of the activation energy, Q, with the QCF HTT is illustrated in Fig. 15. Both Q and R_0 values increased with a rising HTT, but the trend

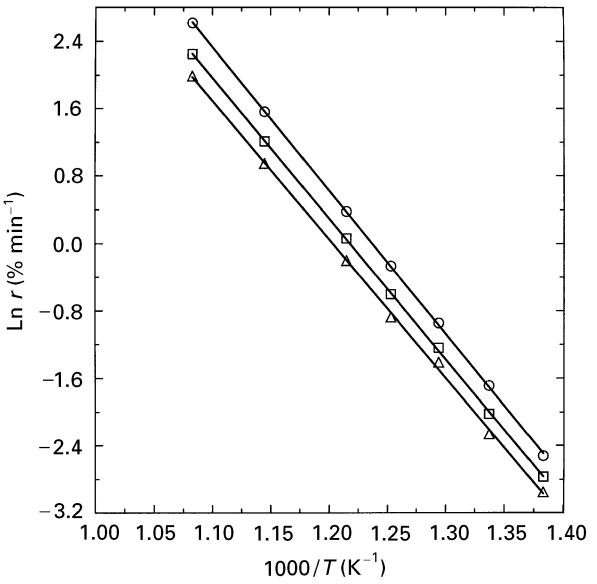

Figure 13 Arrhenius plots for oxidation rate, r, of QCF-650 at 450–650 °C for various BO percentages x: (○) 10%, (□) 25%, (△) 50%.

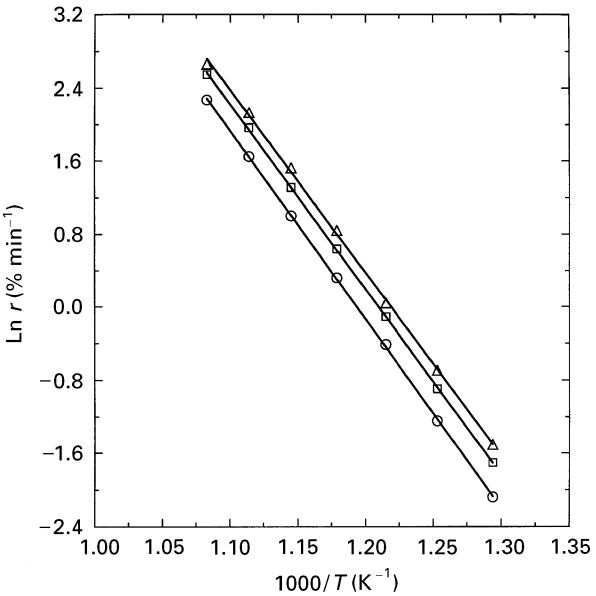

Figure 14 Arrhenius plots for oxidation rate, r, of QCF-950 at 500–650 °C for various BO percentages x: (○) 10%, (□) 25%, (△) 40%.

TABLE III Pre-exponential constants, r_0 and R_0 for various QC fibres

QC fibres	r_0 (10^5 min^{-1}) at x				R_0 (10^5 min^{-1}) at x			
	0%	10%	20%	50%	0%	10%	20%	50%
QCF-400	7.025	5.821	4.681	2.141	7.025	6.486	5.854	4.271
QCF-500	54.04	48.42	43.46	25.35	54.04	53.80	54.33	50.70
QCF-650	272.2	223.4	186.2	137.5	272.2	248.2	232.8	275.0
QCF-800	130.8	461.2	544.4	492.2	130.8	512.4	680.0	984.4
QCF-950	261.5	1064	1465	1510	261.5	1182	1831	3020

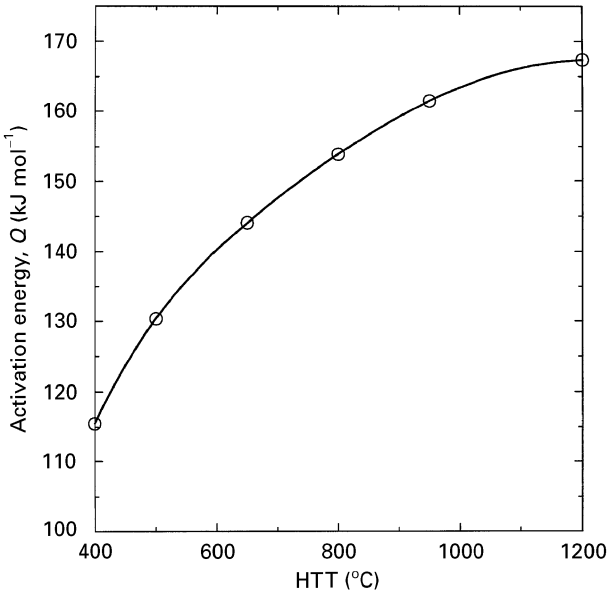

Figure 15 The activation energy of QC fibres as a function of HTT.

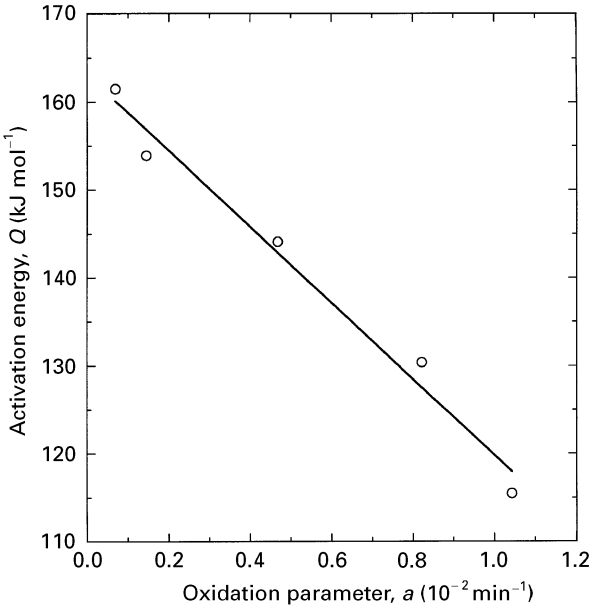

Figure 16 The linear relationship between the activation energy and the oxidation parameter *a*.

gradually levelled off at temperatures above 650 °C. Thus, the activation energy value for the QCF-400 appeared to be 115.8 kJ mol^{-1} and the values for the QCF-500, QCF-650, QCF-800 and QCF-950 increased subsequently. The Q value of carbon fibre, heat treated at 1200 °C, was 167.5 kJ mol^{-1}, which was close to the result reported by Lain *et al.* [17]. Because the Q value plays a more crucial role than the R_0 value within the measured temperature region in determining the oxidation rate, the result indicated that the thermal stability of QC fibres quantitatively increased with an increase in the HTT, particularly when the HTT is below 650 °C. The activation energy, Q, as a function of the oxidation parameter, a, of QC fibres is shown in Fig. 16. The almost linear relationship between Q and a indicates that these two parameters are highly consistent in describing the oxidation behaviour of QC fibres. The high reactivity of the QC fibre at the initial stage ($x = 0$) came out from a small value of the activation energy and vice versa. Thus, the a value was also used quantitatively to evaluate the thermal stability of QC fibres at a specific reaction temperature.

An additional feature being pointed out, is the oxidation mechanism. According to previous studies [18, 19], the oxidation of carbon materials can be divided into several zones, among which the chemical reactions and the diffusions (mass transport) are two major limiting steps. Because the activation energy for the chemical reaction is much higher than that of the diffusion boundary layer (14–16 kJ mol^{-1}), one may conclude that the oxidation of QC fibres at the measured temperature range was mainly controlled by chemical reactions.

3.4. Correlation between oxidation and structural parameters of QC fibres

As discussed earlier, the oxidation behaviour of QC fibres can be classified into two categories. The first one referred to QC fibres which were heat treated at a temperature below 650 °C. Their oxidation rate, r, increased with an increase in the BO percentage x. The so-called auto-acceleration effect occurred in the QC fibres pyrolysed above 650 °C (the second category). The ASA can be used qualitatively to describe the behaviour, but further understanding is needed to evaluate the relationship between the microstructure and oxidation parameters of QC fibres.

The variations in both the activation energy, Q, and the oxidation parameter, a, with the stacking size, L_c, of the QC fibres are illustrated in Fig. 17. Both curves show an almost linear relationship with L_c up to 1.27 nm, the stacking size of the QCF-800, above which the curves levelled- off. The changes actually reflect the two different oxidation mechanisms that the QC fibres followed. At a heat-treatment temperature

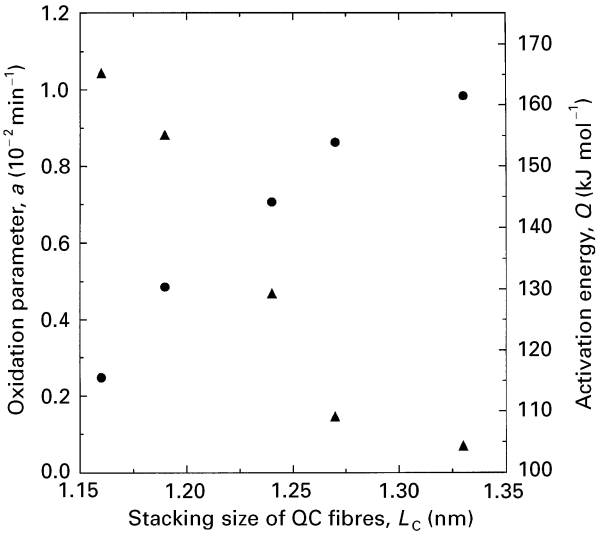

Figure 17 Variations of both (●) activation energy and (▲) oxidation parameter, a, with stacking size.

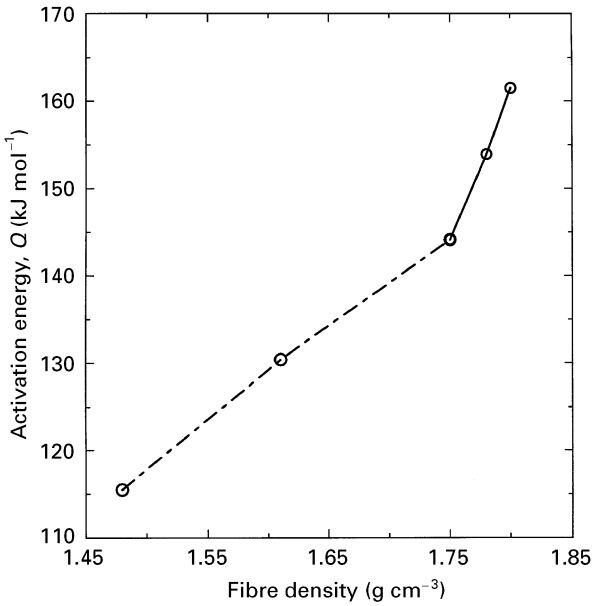

Figure 18 The variation of the activation energy with the density of QC fibres.

below 650 °C, small-size carbon layers were formed with more organic functional groups, such as –OH, =CO and –COOH, etc., connected to the edge carbon atoms [3]. In this imperfect structure, the edge carbon atoms also had unpaired electrons which were available to form bonds with chemo-absorbed oxygen. Therefore, the QC fibre exhibited the high reactivity at the early stage of the oxidation. A longer reaction time would lower concentrations of these organic groups, leading to a decrease in the oxidation rate, r, or the reactivity, R. When the heat-treatment temperature was well above 650 °C, the resulting QCF-800 and QCF-950 would consist of more compact graphite-like structures with extended two-dimensional carbon layers which were less active. The initial reaction rate, r, was thus low. The fused aromatic carbon structure could be broken off with increasing oxidation time to form many smaller species with unpaired σ-electrons, which cause an increased oxidation rate, r, thereafter, or auto-acceleration. Fig. 18 presents the variation of the activation energy with the QCF density, another structural parameter of QC fibres. A similar trend can also be observed, with two different linear regions. The turning point appeared to be at 1.75 g cm^{-3} (the density of the QCF-650). Hence, the data further confirmed that the oxidation behaviour of QC fibres followed two different mechanisms due to the structural change. The transition occurred at the HTT around 650 °C.

4. Conclusions

1. Partially carbonized PAN-based fibres (QC fibres) that are obtained at different heat-treatment temperatures (HTT) exhibited different thermal stability. Both dynamic and isothermal scans by TGA revealed that the oxidation resistance of QC fibres increased with increasing HTT.

2. Both oxidation kinetics data and the data on structural parameters of QC fibres indicated that the oxidation behaviour of QC fibres followed two different mechanisms. An auto-acceleration mechanism was observed for the QC fibre that was pyrolysed at above 650 °C.

3. A model has been developed to describe the oxidation process of QC fibres. The parameters a and b used in the model reflected the thermal stability and the oxidation mechanism in QC fibres, respectively.

4. The activation energy value varied from 115.5–161.5 kJ mol^{-1} for various QC fibres, indicating that oxidation was mainly controlled by the chemical reaction, not by diffusion.

Acknowledgements

Financial support provided by the advanced NSF/Alabama EPSCoR programme is gratefully acknowledged.

References

1. J. G. VENNER and Y. S. KO, *US Pat.* 4938 941 (1990).
2. G. PAN, N. MUTO, M. MIYAYAMA and H. YANAGIDA, *J. Mater. Sci.* **27** (1992) 3497.
3. L. R. ZHAO and B. Z. JANG, *ibid.* **30** (1995) 4535.
4. L. R. ZHAO, J. L. ZHOU and B. Z. JANG, in "Proceedings of the 52nd Annual Technical Conference", San Francisco (The Society of Plastic Engineers, Brookfield, CT, 1994) pp. 2358.
5. B. Z. JANG and L. R. ZHAO, *J. Mater. Res.* **10** (1995) 2449.
6. L. R. ZHAO and B. Z. JANG, *J. Mater. Sci. Lett.* **15** (1996) 99.
7. H. A. GOLDBERG, I. L. KALNIN, C. C. WILLIAMS and I. L. SPAIN, *US Pat.* 4642 664 (1987).
8. G. PAN, N. MUTO, M. MIYAYAMA and H. YANAGIDA, *J. Mater. Sci. Lett.* **12** (1993) 666.
9. N. MUTO, M. MIYAYAMAN, H. YANAGIDA, N. MORI, T. KAJIWARE, Y. IMAI, A. URANO and H. ICHIKAWA, *Sensors Mater.* **2** (1991) 313.
10. M. K. ISMAIL, *Carbon* **29** (1991) 777.
11. K. SAITO and H. OGAWA, in "31st International SAMPE Symposium", edited by J. L. Bauer and R. Dunaetz (Society for the Advancement of Materials and Processing Engineering, Covina, CA, 1986) pp. 1647.
12. B. H. ECKSTEIN, in "18th International SAMPE Technical Conference", edited by J. T. Hoggatt, S. G. Hill and J. C. Johnson (Society for the Advancement of Materials and Processing Engineering, Covina, CA, 1986) pp. 149.

13. B. G. IACOCCA and D. J. DUQUETTE, *J. Mater. Sci.* **28** (1993) 1113.
14. Y. YIN, J. G. P. BINNER and T. E. CROSS, *ibid.* **29** (1994) 2250.
15. E. R. TRUMBAUER, J. R. HELLMANN and L. E. JONES, *Carbon* **30** (1992) 873.
16. W. S. HORTON, in "Proceedings of the 5th Conference on Carbon", Pennsylvania State University (Symposium Publication Division, Pergamon Press, New York, 1961) vol. 2, pp. 233.
17. N. R. LAIN, F. J. VASTOLA and P. L. WALKER, *ibid.* pp. 211.
18. P. L. WALKER, F. RUSINKO and L. G. AUSTIN, *Adv. Catal.* **11** (1959) 133.
19. E. N. FULL, P. D. SCHETTLER and J. C. GIDDINGS, *Ind. Eng. Chem.* **58** (1966) 19.

Received 29 August
and accepted 30 October 1996